J. Applied Membrane Science & Technology, Vol. 27, No. 1, April 2023, 47–61

Effect of Diameter of Carbon Nanotubes in Nanocomposite Membrane for Methyl Orange Dye Removal

Kah Chun Ho[a*], Jin Heng Lim[a], Aida Isma Mohd Idris[a],
Yeit Haan Teow[b] & Nii Chien Ng[a]

[a]Centre for Water Research, Faculty of Engineering and the Built Environment, SEGi University, Jalan Teknologi, Kota Damansara, 47810 Petaling Jaya, Selangor Darul Ehsan, Malaysia
[b]Department of Chemical and Process Engineering, Faculty of Engineering and Built Environment, Universiti Kebangsaan Malaysia, 43600, UKM Bangi, Selangor Darul Ehsan, Malaysia

Submitted: 18/1/2023. Revised edition: 14/2/2023. Accepted: 14/2/2023. Available online: 20/3/2023

ABSTRACT

It is worth noticing that structure of nanomaterials affects the membrane performance, however, the effect of diameter of multiwalled carbon nanotubes (MWCNTs) has not been discussed in the past. This research aims to investigate the effect of diameter of MWCNTs on the performance of graphene oxide (GO)/ MWCNTs nanocomposite membrane for methyl orange dye removal. MWCNTs with different diameters (12-15 nm, 30-50 nm) with the same length (< 10 μm) are used to synthesize the nanocomposite membrane. The characteristics of the synthesized nanocomposite membrane were determined by surface hydrophilicity, pore size and porosity, zeta potential, and Fourier-transfer infrared (FTIR) spectroscopy. Besides, the membrane performance was evaluated by the water permeability test, dye rejection test, and antifouling test. The result showed that pure MWCNTs (30-50 nm) nanocomposite membrane (M2b) has the best performance among the synthesized membrane. The dye rejection of M2b membrane reached 86.77% and the normalized flux was approximately 0.82. Lower dye rejection (83.37%) and normalized flux (0.76) were attained by M2a membrane with smaller diameter MWCNTs (12-15 nm). This was due to M2b membrane having a smaller pore size (0.032 nm), which helped reduce the tendency of dye to pass through the membrane. Besides, M2b membrane has a more negative surface charge (-10.93 mV) that produces larger repulsion force, resulting in more dye being rejected. In conclusion, the performance of the synthesized nanocomposite membrane particularly antifouling properties can be enhanced with the addition of MWCNTs with larger diameter.

Keywords: Diameter of nanotubes; graphene oxide, membrane antifouling, multiwalled carbon nanotubes, nanocomposite membrane

1.0 INTRODUCTION

Plenty of wastewater was produced by industries due to high water usage and caused water scarcity, which is the world's top environmental problems faced by human beings [1]. Textile wastewater produced from textile industries is one of the major contributors to water pollution [2]. During the past few decades, the development of membrane technologies has gained much attention. It is used in the wastewater treatment process due to few reasons including small footprint, low chemical usage, and high efficiency in separation process [3]. However, it would face an inevitable problem, that is membrane fouling [4].

* Corresponding to: Kah Chun Ho (email: hokahchun@segi.edu.my)
DOI: https://doi.org/10.11113/amst.v27n1.262

There were few approaches to mitigate the membrane fouling issue. The development of the antifouling membrane by reducing the interaction of the membrane surface with the foulants was introduced. Graphene oxide (GO) was a monolayer with a highly oxidative form and it consists of different oxygen-containing functional groups, including hydroxyl, carbonyl, carboxyl, and epoxy groups [5]. Du *et al*. [6] found out that by increasing the content of the GO - zinc sulfide (GO-ZnS) in the polyvinylidene fluoride (PVDF) membrane, the contact angle of the membrane would decrease, and this showed that the hydrophilicity of the membrane improved. Carbon nanotubes (CNTs) including single and multiwalled were one of the forms of carbon nanomaterials and it had been drawing attention in research nowadays [7]. Bai *et al*. [8] used functionalized multiwalled CNTs (MWCNTs) to modify ultrafiltration (UF) membrane and the result showed that the antifouling properties of the modified membrane were improved compared with the virgin membrane.

The diameter of MWCNTs is an important factor to be investigated to enhance the performance of nanocomposite membranes further. Jia *et al*. [9] reported that the optimum diameter of the CNT is approximately 1 nm. The larger the diameter of CNTs would have lower water flux due to the water viscosity increase when the diameter increase. However, the water transportation through the CNTs is fast because CNTs having smooth surfaces. The previous research reported that thin long MWCNTs tends to cluster causing the fraction of isolated nanotube to be low [10]. The agglomeration of the MWCNTs brings negative effects to the membrane. Yang *et al*. [10] found that the distribution of the MWCNTs with large diameter is more uniform in the polymer matrix compared to a smaller diameter. This is agreed by Kim *et al*. [11] where their studies reported that the tendency of aggregation of CNTs with larger diameter is less compared to the CNTs with smaller diameter. This is related to the short and thick nanotube with low flexibility and small surface area [12]. This showed that the dispersibility of the large diameter MWCNTs is better. Hence, it reduces the agglomeration of the MWCNTs and improves the specific surface area [7]. In addition, Ajmani *et al*. [13] reported a large diameter of MWCNTs was more effective in removing large organic macromolecules causing fouling. Alsawat *et al*. [14] used (RosB)-2 molecules, a type of dye molecules to determine the transport properties of the MWCNTs with different diameter. The result showed that the diffusional flux of MWCNTs with smaller diameter was higher than MWCNTs with larger diameter. This was due to the interactions between the dye molecules with the CNTs increase when the diameter was smaller. Past research also showed the synergistic effect of GO/MWCNTs nanocomposite membrane owing to the stable three-dimensional network structure formed by GO and MWCNTs through $\pi-\pi^*$ interactions [15, 16].

However, up to date, the effect of diameter of MWCNTs in GO/MWCNTs nanocomposite membrane has not been reported. In that case, the effect of the diameter of the MWCNTs in GO/MWCNTs nanocomposite membrane should be studied to enhance the performance of the membrane further. This research investigated the effect of diameter of MWCNTs towards the GO/MWCNTs nanocomposite membrane. First objective of this research was to synthesize GO/MWCNTs nanocomposite membrane by using direct blending method. Two different MWCNTs diameters (12-15 nm, 30-50 nm) with the same length (<10 μm) were used to determine the effect of diameter. The weight ratio of carbon nanomaterials (GO: MWCNTs) was manipulated at 0:0, 0:10, 5:5, and 10:0 [17]. The performance of the

synthesized nanocomposite membrane was conducted including membrane permeability test, dye rejection test and also antifouling test. Methyl orange was used as dye for the dye rejection test.

2.0 METHODS

2.1 Materials

GO sheet was used in membrane modification and obtained from previous research. Two different diameters of MWCNTs (12-15 nm, 30-50 nm) with same length (<10 µm) were used to study the effect of diameter in this research and were purchased from NanoAmor, USA. Polyvinylidene fluoride (PVDF) powder was obtained from ThermoFisher Scientific, USA and was used to synthesize membrane. N-N-di-methylacetamide (DMAc) (assay GC area > 99%) was supplied by Merck Co., Germany was used as solvent to dissolve the PVDF. Methyl orange was the dye used in the evaluation of the membrane performance and it was purchased from Alfa Aesar, USA.

2.2 Membrane Synthesis

The GO/MWCNTs nanocomposite membrane was synthesized using a direct blending method similar to the method reported by Ho *et al*. [17]. The GO and MWCNTs would be integrated into the membrane matrices. First, GO and MWCNTs (1 wt%) were dispersed into DMAc under sonification using an ultrasonicator Symphony 97043-932 (Avantor Inc., USA). After 30 minutes, PVDF was added to the carbon nanomaterials suspension. The mixture was stirred for 4 hours at 250 rpm and 65 ºC. Then, the solution was stirred for another 4 hours at 250 rpm and 40 ºC to make sure PVDF was completely dissolved in the mixture. The solution was kept overnight in a desiccator to remove the trapped air bubble in the membrane polymer solution. After that, the membrane polymer solution was cast on a flat non-woven polyester membrane support (CU414 Opti, Neenah US) affixed on a glass plate with the help of a film applicator and bar coater. Membrane thickness was fixed at 200 µm using feeler gauge. The glass plate containing the membrane polymer solution was then immersed into RO water bath for one day. This was to ensure the solidification of the membrane was completely done. Finally, the synthesized membrane was taken out from the water bath and stored in fresh RO water. Table 1 shows the membrane formulation in studying the effect of diameter of the MWCNTs toward GO/MWCNTs nanocomposite membrane.

Table 1 Membrane formulation in studying the effect of diameter of the MWCNTs toward membrane

Membrane	Diameter of MWCNTs (nm)	Carbon nanomaterial ratio (g/g)	
		GO	MWCNTs
M0	-	0	0
M1	-	10	0
M2a	12 - 15	0	10
M2b	30-50	0	10
M3a	12-15	5	5
M3b	30-50	5	5

2.3 Membrane Characteristics

2.3.1 Surface Hydrophilicity

The surface hydrophilicity of the membrane was determined by contact angle with a contact-angle meter [18]. The membrane sample was affixed tightly onto a glass slide with the help of double side tape. Then, a water droplet of approximately 13 µL was dropped on the membrane surface and the view was obtained by using a high-speed camera of the contact angle meter at frequency of 100 pcs/s. The image obtained was interpreted using Drop Shape Analysis (DSA) software to compute the contact angle of the membrane surface. The contact angle was measured at three different spots to minimize the experimental error.

2.3.2 Pore Size and Porosity

The gravimetric method was used to determine the membrane porosity [19]. First, the membrane was immersed in RO water for 12 hours. Then, the membrane was cut into small pieces. The dimension of the membrane piece was approximate 1 cm × 1 cm. The droplets on the membrane were wiped gently by using filter paper and weighed. Then, the membrane was dried at 50 °C for 24 hours and weighed again. The porosity of membrane was determined using Equation 1 [20].

$$\varepsilon = \frac{\frac{w_1 - w_2}{\rho_w}}{\frac{w_1 - w_2}{\rho_w} + \frac{w_2}{\rho_p}} \quad (1)$$

where, ε = membrane porosity (%), w_1 and w_2 = wet and dry weight of the membrane (g), ρ_w = density of distilled water (0.998 g/mL), and ρ_p = density of polymer (PVDF = 1.765 g/mL at 25 °C).

The membrane mean pore size was determined using the Guerout-Elford-Ferry equation as shown in Equation 2 [19].

$$r_m = \sqrt{\frac{(2.90 - 1.75\varepsilon)8V\mu\delta}{\varepsilon PA}} \quad (2)$$

where, r_m = membrane mean pore radius (m), ε = membrane porosity (%), V = water flow rate, (m^3/s), µ = dynamic viscosity of water at 25 °C (8.9×10^{-4} Pa. s), δ = membrane thickness (m), P = operating pressure (Pa), and A = membrane area (m^2).

2.3.3 Surface Charge

Membrane surface charge was determined by zeta potential measurement using Zeta Sizer, Nano-ZS. The membrane sample with dimension 1 cm × 1 cm was affixed on the zeta potential cell and immersed in 0.1 mM NaCl together with 300–350 nm latex particles at neutral pH. Membrane surface charge was assessed by the mobility of latex particles at multiple distances away from the membrane surface upon applying an electric field at 25 V/cm [17].

2.3.4 Functional Groups

FTIR spectrometer Spectrum 100 (PerkinElmer Inc., USA) was used to determine the functional groups on the GO/MWCNTs nanocomposite membrane [21]. The operating wavelength was in the range of 500 cm^{-1} to 4000 cm^{-1}.

2.4 Membrane Performance

2.4.1 Membrane Permeability Test

First, the membrane was pressurized at a constant pressure of 1.5 bar for 15 minutes to minimize the impact of compaction [22]. Transmembrane pressure (TMP) of 0.5, 1.0, and 1.5 bar were applied for 10 minutes for each pressure to conduct the membrane permeability test. The membrane

permeate flux is obtained by Equation 3 and the membrane permeability is determined by the gradient of permeate flux against TMP [23].

$$J = \frac{\Delta V}{A\Delta t} \quad (3)$$

where, J = permeate flux (L/m^2.h), ΔV = permeate volume (L), A = effective membrane filtration area (m^2), Δt = permeation time (h).

2.4.2 Dye Rejection Test

The ability of the membranes towards dye rejection was tested using a 30 mg/L solution of methyl orange at 1 bar in a stirred ultrafiltration cell MA-01730 (Millipore, U.S.) for 15 minutes. The dye rejection was determined using Equation 4 [24].

$$R = (1 - \frac{C_p}{C_f}) \times 100 \quad (4)$$

where, R = membrane rejection (%), C_p = concentration of permeate (mg/L), C_f = the concentration of feed solution (mg/L)

2.4.3 Membrane Antifouling Test

This membrane antifouling test was conducted using the 30 mg/L of dye solution under 10 minutes of a dead-end membrane filtration system. The operating pressure and temperature were fixed at 1 bar and 25 °C, respectively [25]. Normalized flux was obtained by using Equation 5.

$$Normalized\ Flux = \frac{J_1}{J} \quad (5)$$

where, J_1 = permeate flux for membrane filtration system using 30 mg/L dye solution as feed, J = permeate flux of the membrane at the first minute.

3.0 RESULTS AND DISCUSSION

3.1 Membrane Characteristics

3.1.1 Surface Hydrophilicity

Table 2 shows the contact angle result for the synthesized membrane. The result showed that the M1 membrane has the highest contact angle meanwhile the M2a membrane has the lowest contact angle value. The images of water droplet on M0, M1, and M2a membranes were shown in Figure 1.

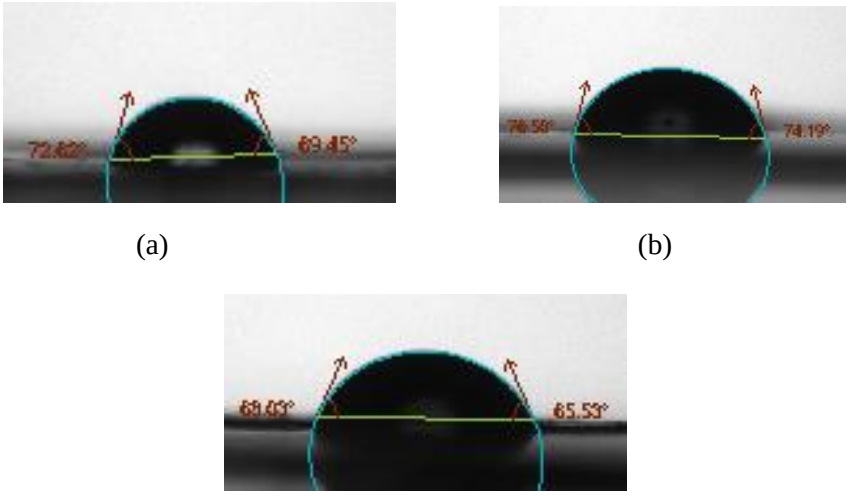

Figure 1 Images of water droplets on (a) M0, (b) M1, and (c) M2a membrane

Table 2 Contact angle of synthesized membrane

Membrane	Contact Angle (°)
M0	68.99 ± 0.55
M1	72.64 ± 1.99
M2a	68.62 ± 1.68
M2b	70.41 ± 0.05
M3a	69.12 ± 0.53
M3b	69.92 ± 1.60

The contact angle value for the M0 membrane was 68.99° which was the second-lowest of all the membranes. After incorporating the GO into the membrane, the contact angle of membrane increases. This was probably due to the concentration of GO being too high causing GO to partially agglomerate [26]. The result showed that for pure MWCNTs nanocomposite membrane, the contact angle value of M2b membrane was greater than M2a membrane. The trend was the same for GO/MWCNTs nanocomposite membrane (M3a and M3b). This result was similar as the result reported by Mollhosseini *et al*. [27]. Larger nanoparticle size would create a membrane that has a larger contact angle value. This situation happened probably due to the surface roughness of the membrane increasing. Air was trapped and formed a gap between the membrane surface and water droplet, causing the water droplet to not contact directly with the membrane surface, resulting in increased water contact angle [17].

3.1.2 Pore Size and Porosity

Table 3 shows the result of pore size and porosity for the synthesized membranes. The pore size of all synthesized membranes was in the range of 0.019 -0.04 μm. Hence it could be considered as ultrafiltration (UF) membrane (0.003 – 0.1 μm) [28]. M3b membrane has the largest pore size while M1 membrane has the smallest pore size. By adding the MWCNTs into the PVDF membrane (M2a and M2b), the pore size increased due to the acceleration of the diffusion rate between water and DMAc resulting in a bigger pore size [29]. The pore size of M2a membrane was bigger than M2b membrane and this was probably due MWCNTs with smaller diameters tend to agglomerate compared to the larger diameter [11]. This is consistent with past studies that reported that the tendency of aggregation of CNTs with larger diameter is less compared to the CNTs with smaller diameter [11]. This is because the short and thick nanotube has low flexibility and small surface area [12]. If the agglomerate happened, the pore structure of the membrane would be affected and become larger.

For GO/MWCNTs nanocomposite membranes (M3a and M3b), the agglomeration was less significant due to the addition of GO reducing the tendency of agglomeration of MWCNTs [30]. This was probably due to the presence of oxygen-containing groups on the GO that improved the dispersibility of the MWCNTs. The pore size of M3b membrane was larger than the M3a membrane was probably due to the larger diameter MWCNTs formed larger porous structures in the membrane polymer matrix during the phase inversion process compared to the smaller diameter of MWCNTs [13]. For the porosity, M3a membrane showed the highest value and the lowest value was M0 membrane. In general, the porosity of the nanocomposite membrane was higher compared to the pure PVDF membrane. This was due to the hydrophilicity properties of MWNCTs that increase the diffusion rate between water and DMAc during the phase inversion process [29].

Table 3 Pore size and porosity of synthesized membrane

Membrane	Pore Size (µm)	Porosity (%)
M0	0.022	50.55
M1	0.019	55.22
M2a	0.039	57.81
M2b	0.032	55.32
M3a	0.030	59.11
M3b	0.040	52.30

3.1.3 Surface Charge

Figure 2 shows the result of zeta potential for the synthesized membranes. M3a membrane has the lowest zeta potential and M1 membrane have the highest zeta potential. The result shows that M0 membrane has the second-lowest negative charge among all synthesized membranes. The zeta potential for M2a membrane was greater than M2b membrane. This result showed that the negative charged was lower for the larger diameter of MWCNTs than the smaller diameter. This result showed the same trend as the studies conducted by Zhang *et al*. [31]. This was probably due to the zeta potential would be affected by the dispersibility of the nanomaterials [32]. Since the dispersibility of larger diameter MWCNTs was better compared to the smaller diameter, the zeta potential of M2b membrane was lower than M2a. The reason for M3a membrane having the highest potential was the negatively- charged –COOH functional groups present on the GO nanosheets [17]. M3b membrane has high zeta potential value was probably due to the partial agglomeration of GO since the dispersibility would affect the zeta potential value [26].

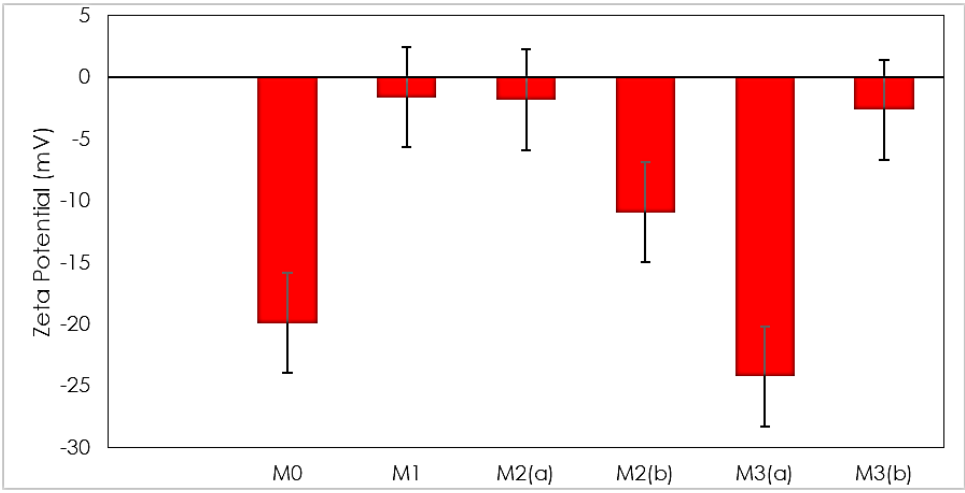

Figure 2 Zeta potential of synthesized membrane

3.1.4 Functional Groups

Figure 3 shows the FTIR result of the synthesized membranes. From the result, a peak of the wavelength of 1717 cm^{-1} could be observed for all synthesized membranes. This peak was contributed by carboxyl (C=O) groups. Besides, peaks of wavelength of 1248 cm^{-1} and 1101 cm^{-1} was shown and this represented the presence of the epoxy (C-O-C) and alkoxy (C-O) groups, respectively [21]. The population of C=O group of the M1 membrane was higher than M0 membrane since the transmittance peak was lower. For the

M2a and M2b membrane, the presence of C-O-C group was more significant. The trend was similar for the GO/MWCNTs nanocomposite membrane. In addition, there was a peak found at 1410 cm^{-1} for M3b membrane and this was probably due to the β- phase of the PVDF [19].

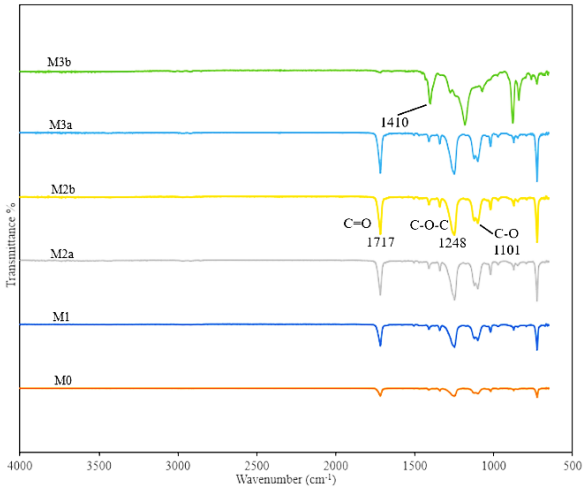

Figure 3 FTIR spectrum of the synthesized membrane

3.2 Membrane Performance

3.2.1 Membrane Permeability

Figure 4 shows the result for the water permeability test of the synthesized membrane. The result showed that the membrane with the highest permeability was M3b membrane meanwhile M1 membrane has the lowest water permeability. The membrane permeability for the M0 membrane was considered low compared to the membrane modified by MWCNTs and GO/MWCNTs. The pore size result could support this result. The pore size of the modified membrane (0.030 - 0.04 μm) was much larger compared to the pure PVDF membrane (0.022 μm). Hence, more water molecules could pass through the membrane. Besides, MWCNTs were hydrophilic resulting in it could attract the water molecule inside the polymer matrix and helping the water molecule to permeate easily. The water permeability of M1 membrane was the lowest among the synthesized membrane. The pore size of the M1 membrane was the smallest contributing to the lowest water permeability. M2a membrane has higher water permeability (139.33 $L/m^2.h.bar$) than M2b membrane (108.40 $L/m^2.h.bar$) since the pore size of M2a membrane was larger than M2b membrane. Besides, the contact angle for the M2a membrane was smaller than the M2b membrane. Hence, the hydrophilicity of M2a membrane was higher than the M2b membrane. Larger diameter of MWCNTs has lower water flux could probably due to the membrane polymer solution viscosity increasing when the diameter of the MWCNTs increased [33].

For the water permeability of GO/MWCNTs nanocomposite membrane, the membrane with a larger diameter (M3b) showed better water permeability than the smaller diameter (M3a). This result showed the same trend as the pore size that M3b membrane has larger pore size. However, the contact angle result showed that the hydrophilicity of M3a

membrane was better than M3b membrane. This was probably due to the pore size of the membrane having higher impact on the water permeability compared to the water contact angle [34]. Moreover, when the increase in MWCNTs diameter, more water molecules were filtered resulting in increased water permeability [35]. By comparing the synthesized membrane, M3b has the best performance in the water permeability test. Thomas and Corry [36] obtained the same result as this research showing that the permeability increased with larger diameter of MWCNTs used in membrane modification.

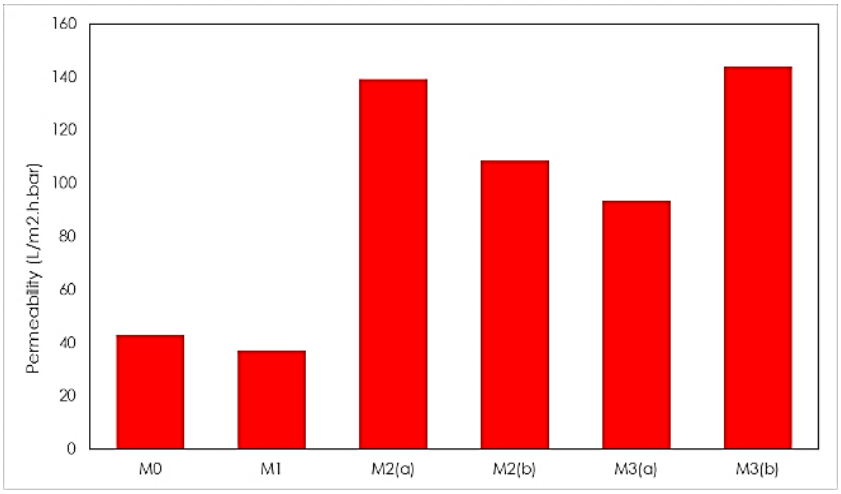

Figure 4 Water permeability result of synthesized membrane

3.2.2 Dye Rejection Test

Figure 5 shows the dye rejection result for all synthesized membranes. M2b membrane has the highest dye rejection meanwhile M3b membrane has the lowest dye rejection among the synthesized membrane. The dye rejection for M0 membrane and M1 membrane could be considered similar because there was no significant difference between the dye rejection values. This was probably due to the pore size of M0 membrane and M1 membrane have not big difference, which were 0.022 μm and 0.019 μm, respectively. For the MWCNTs nanocomposite membrane, the dye rejection result for the M2b membrane was higher compared to M2a membrane. This result was supported by the surface charge of the membrane. Since methyl orange is negatively charged, M2b membrane with a more negative surface charge has a larger repulsion force, resulting in more dye being rejected. This result was supported by the result reported by [37] which by using a larger nanoparticle size in membrane modification, the dye rejection would increase. Besides, M2b membrane has smaller pore size compared to M2a membrane and this also helped to reduce the tendency of dye to pass through the membrane. Zhang *et al*. [31] get the same result as this research showing that the smaller pore size of the membrane has a higher selectivity.

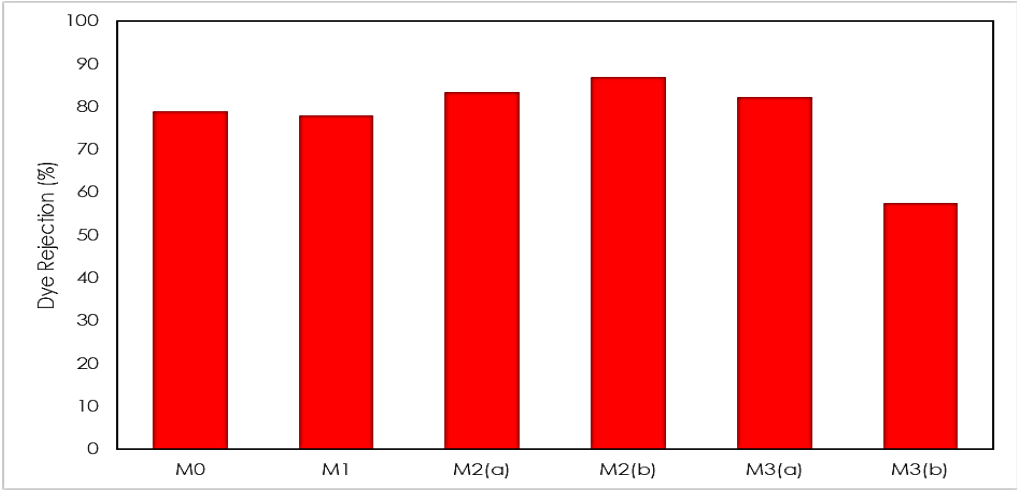

Figure 5 Dye rejection test

For GO/MWCNTs membrane, the dye rejection of M3a membrane was higher than M3b membrane. However, this result was different from the result expected which by using larger nanoparticle size in modification of membrane, the dye rejection would increase [37]. This was probably due to the lower zeta potential in the M3a membrane (-24.2 mV) compared to M3a membrane (-2.61 mV). The performance of the M3b membrane was not as expected, it could also reject the dye until 57.4%. However, the result was considered acceptable because the size of the methyl orange (0.006-0.008 μm) was much smaller than the pore size of M3b membrane (0.040 μm) but it could still rejection above 50% [38].

3.2.3 Membrane Antifouling Test

Figure 6 shows the result of the antifouling test of the synthesized membrane. The result showed that the M2b membrane has the highest normalized flux which indicates the best antifouling characteristic. Meanwhile, M0 membrane has the lowest normalized flux among the synthesized membrane. The normalized flux was increased by about 9.47% when GO was used to modify the PVDF membrane. For pure MWCNTs membrane, M2b membrane showed higher normalized flux approximately 8.22 % compared to M2a membrane. This was supported by the surface charged result which the zeta potential of the M2b membrane (-10.93 mV) was lower than the M2a membrane (-1.81 mV). Since the methyl orange was negatively charged, the surface repulsion force towards the dye for the M2b membrane was greater resulting in reduced the tendency of membrane fouling [39].

For the GO/MWCNTs membrane, M3b membrane showed better normalized flux, 1.96% higher compared to the M3a membrane. This result was probably due to the pore size of the membrane. Since the pore size of M3b membrane was larger compared to M3a membrane, the dye would not block the membrane pore easily, hence the antifouling property of the M3b was enhanced [29].

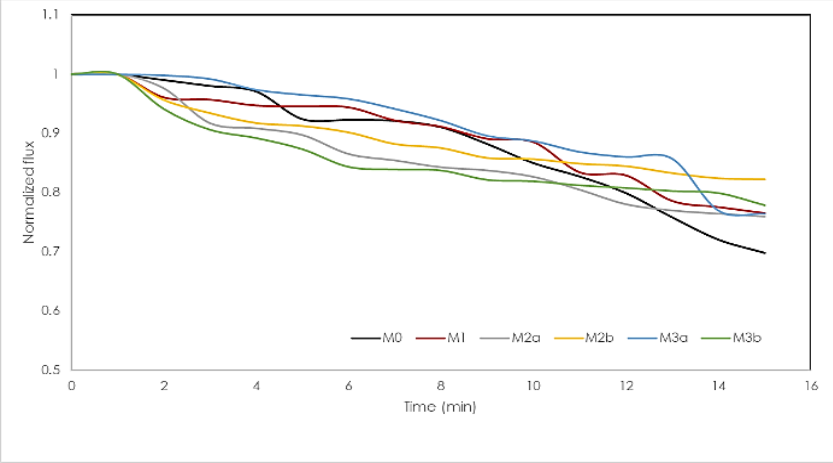

Figure 6 Result of antifouling test of synthesized membrane

4.0 CONCLUSION

This project was carried out to investigate the effect of diameter of MWCNTs on the performance of GO/MWCNTs nanocomposite membrane for methyl orange dye removal. MWCNTs with different diameters (12-15 nm, 30-50 nm) with the same length (< 10 µm) of MWCNTs were used to synthesize the nanocomposite membrane. It could be identified that the membrane with larger MWCNTs diameter (M2b) has the best performance compared to other synthesized membrane. This was due to the dye rejection and also the normalized flux of the M2b membrane was the highest among the synthesized membrane. This is because the dispersibility of the large diameter MWCNTs is better. This proves that by incorporating larger diameter of MWCNTs into the membrane polymer matrix, the performance of the modified membrane would be improved compared to the small diameter of MWCNTs due to the enhanced membrane characteristics such as zeta potential.

ACKNOWLEDGEMENT

This research is fully supported by SEGi Internal Research Fund grant, SEGiIRF/2022-Q1/FoEBEIT/002. The authors fully acknowledged Department of Chemical and Process Engineering of UKM for laboratory analysis.

REFERENCES

[1] M. Elimelech. 2006. The global challenge for adequate and safe water. *Journal of Water Supply: Research and Technology - AQUA*. 55: 3-10. https://doi.org/10.2166/aqua.2005.064.

[2] D. A. Yaseen, M. Scholz. 2019. Textile dye wastewater characteristics and constituents of synthetic effluents: a critical review. *International Journal of Environmental Science and Technology*. 16: 1193-1226. https://doi.org/10.1007/s13762-018-2130-z.

[3] J. R. Werber, C. O. Osuji, M. Elimelech. 2016. Materials for next-generation desalination and water purification membranes. *Nat Rev Mater*. 1. https://doi.org/10.1038/natrevmats.2016.18.

[4] H. Sharifi, P. A. Moghaddam, S. Jafarmadar, A. M. Nikbakht, A. Hosainpour. 2022. Fouling

performance of a horizontal corrugated tube due to air injection, international journal of engineering. *Transactions B: Applications.* 35: 1074-1081. https://doi.org/10.5829/ije.2022.35.05b.22.

[5] M. R. Halvaeyfar, S. M. Mirhosseini, E. Zeighami, A. H. Joshaghani. 2022. Experimental study on bonding CFRP to fiber concrete beam considering the effect of using nanographene oxide in improving the mechanical properties of polyamine resin. *International Journal of Engineering, Transactions B: Applications*. 35. https://doi.org/10.5829/IJE.2022.35.08B.09.

[6] J. Du, N. Li, Y. Tian, J. Zhang, W. Zuo. 2020. Preparation of PVDF membrane blended with graphene oxide-zinc sulfide (GO-ZnS) nanocomposite for improving the anti-fouling property. *J Photochem Photobiol A Chem.* 400: 112694. https://doi.org/10.1016/j.jphotochem.2020.112694.

[7] S. M. Abdelbasir, A. E. Shalan. 2019. An overview of nanomaterials for industrial wastewater treatment. *Korean Journal of Chemical Engineering.* 36: 1209-1225. https://doi.org/10.1007/s11814-019-0306-y.

[8] L. Bai, H. Liang, J. Crittenden, F. Qu, A. Ding, J. Ma, X. Du, S. Guo, G. Li. 2015. Surface modification of UF membranes with functionalized MWCNTs to control membrane fouling by NOM fractions. *J Memb Sci.* 492: 400-411. https://doi.org/10.1016/j.memsci.2015.06.006.

[9] Y. X. Jia, H. L. Li, M. Wang, L. Y. Wu, Y. D. Hu. 2010. Carbon nanotube: Possible candidate for forward osmosis. Sep Purif Technol. 75: 55-60. https://doi.org/10.1016/j.seppur.2010.07.011.

[10] Z. Yang, H. Peng, W. Wang, T. Liu. 2010. Crystallization behavior of poly(ε-caprolactone)/layered double hydroxide nanocomposites. *J Appl Polym Sci.* 116: 2658-2667. https://doi.org/10.1002/app.

[11] K. J. Kim, M. Y. Huh, W. S. Kim, J. H. Song, H. S. Lee, J. Y. Kim, S. R. Lee, W. S. Seo, S. M. Yang, Y. S. Park. 2018. The effect of carbon nanotube diameter on the electrical, thermal, and mechanical properties of polymer composites. *Carbon Letters.* 26: 95-101. https://doi.org/10.5714/CL.2018.26.095.

[12] I. Dubnikova, E. Kuvardina, V. Krasheninnikov, S. Lomakin, I. Tchmutin, S. Kuznetsov. 2010. The effect of multiwalled carbon nanotube dimensions on the morphology, mechanical, and electrical properties of melt mixed polypropylene-based composites. *J Appl Polym Sci.* 117: 259-272. https://doi.org/10.1002/app.31979.

[13] G. S. Ajmani, D. Goodwin, K. Marsh, D. H. Fairbrother, K. J. Schwab, J. G. Jacangelo, H. Huang. 2012. Modification of low pressure membranes with carbon nanotube layers for fouling control. *Water Res*. 46: 5645-5654. https://doi.org/10.1016/j.watres.2012.07.059.

[14] M. Alsawat, T. Altalhi, T. Kumeria, A. Santos, D. Losic.

2015. Carbon nanotube-nanoporous anodic alumina composite membranes with controllable inner diameters and surface chemistry: Influence on molecular transport and chemical selectivity. *Carbon N Y.* 93: 681-692. https://doi.org/10.1016/j.carbon.2015.05.090.

[15] Y. M. Chen, H. Kah Chun, M. K. Chan, Y. H. Teow, M. Aida Isma. 2022. Optimization of Antifouling Properties of Mixed Matrix Membrane Synthesized via in-situ Colloidal Precipitation. *Journal of Membrane Science and Research.*

[16] C. Z. Lee, H. Kah Chun, M. K. Chan, Y. H. Teow. 2022. Effect of Carbon Nanomaterials Concentration in Nanocomposite Membrane for Methyl Blue Dye Removal. *J Teknol.* 84: 19-27. https://doi.org/10.11113/jurnalteknologi.v84.18277.

[17] K. C. Ho, Y. H. Teow, A. W. Mohammad, W. L. Ang, P. H. Lee. 2018. Development of graphene oxide (GO)/multi-walled carbon nanotubes (MWCNTs) nanocomposite conductive membranes for electrically enhanced fouling mitigation. *J Memb Sci*. 552: 189-201. https://doi.org/10.1016/j.memsci.2018.02.001.

[18] G. Yang, Z. Xie, M. Cran, D. Ng, S. Gray. 2019. Enhanced desalination performance of poly (vinyl alcohol)/carbon nanotube composite pervaporation membranes via interfacial engineering. *J Memb Sci*. 579: 40-51. https://doi.org/10.1016/j.memsci.2019.02.034.

[19] M. K. Chan, C. S. Ong, P. Kumaran. 2018. Development and characterization of glycerol coating on the PAN/PVDF composite membranes. *IOP Conf Ser Mater Sci Eng*. 458. https://doi.org/10.1088/1757-899X/458/1/012006.

[20] Y. H. Teow, Shah. Mubassir, K. C. Ho, A. W. Mohammad. 2018. A study on membrane technology for surface water treatment : Synthesis, characterization and performance test. *Membrane Water Treatment*. 2: 69-77. https://doi.org/10.12989/mwt.2018.9.2.069.

[21] N. C. Homem, N. de Camargo Lima Beluci, S. Amorim, R. Reis, A. M. S. Vieira, M. F. Vieira, R. Bergamasco, M. T. P. Amorim. 2019. Surface modification of a polyethersulfone microfiltration membrane with graphene oxide for reactive dyes removal. *Appl Surf Sci.* 486: 499-507. https://doi.org/10.1016/j.apsusc.2019.04.276.

[22] A. Volkov, R. Federation, R. Academy. 2020. *Encyclopedia of Membranes*. 1-2. https://doi.org/10.1007/978-3-642-40872-4.

[23] S. H. Maruf, L. Wang, A. R. Greenberg, J. Pellegrino, Y. Ding. 2013. Use of nanoimprinted surface patterns to mitigate colloidal deposition on ultrafiltration membranes. *J Memb Sci.* 428: 598-607. https://doi.org/10.1016/j.memsci.2012.10.059.

[24] Z. Rahimi, A. A. Zinatizadeh, S. Zinadini, M. C. M. van Loosdrecht. 2020. β-cyclodextrin functionalized MWCNTs as a promising antifouling agent in fabrication

of composite nanofiltration membranes. *Sep Purif Technol.* 247. https://doi.org/10.1016/j.seppur.2020.116979.

[25] N. Aryanti, F. K. I. Sandria, R. H. Putriadi, D. H. Wardhani. 2017 .Evaluation of micellar-enhanced ultrafiltration (MEUF) membrane for dye removal of synthetic Remazol dye wastewater. *Engineering Journal.* 21: 23-35. https://doi.org/10.4186/ej.2017.21.3.23.

[26] D. Ji, C. Xiao, S. An, J. Zhao, J. Hao, K. Chen. 2019. Preparation of high-flux PSF/GO loose nanofiltration hollow fiber membranes with dense-loose structure for treating textile wastewater. *Chemical Engineering Journal.* 33-42. https://doi.org/10.1016/j.cej.2019.01.111.

[27] A. Mollahosseini, A. Rahimpour, M. Jahamshahi, M. Peyravi, M. Khavarpour. 2012. The effect of silver nanoparticle size on performance and antibacteriality of polysulfone ultrafiltration membrane. *Desalination*. 306: 41-50. https://doi.org/10.1016/j.desal.2012.08.035.

[28] S. Vishali, E. Kavitha. 2021. Application of membrane-based hybrid process on paint industry wastewater treatment. *Membrane-Based Hybrid Processes for Wastewater Treatment*. 97-117. https://doi.org/10.1016/b978-0-12-823804-2.00016-1.

[29] B. Hudaib, V. Gomes, J. Shi, C. Zhou, Z. Liu. 2018. Poly (vinylidene fluoride)/polyaniline/MWCNT nanocomposite ultrafiltration membrane for natural organic matter removal. *Sep Purif Technol.* 190: 143-155. https://doi.org/10.1016/j.seppur.2017.08.026.

[30] A. S. Adeleye, J. R. Conway, K. Garner, Y. Huang, Y. Su, A. A. Keller. 2016. Engineered nanomaterials for water treatment and remediation: Costs, benefits, and applicability. *Chemical Engineering Journal*. 286: 640-662. https://doi.org/10.1016/j.cej.2015.10.105.

[31] J. Zhang, Z. Wang, Q. Wang, C. Pan, Z. Wu. 2017. Comparison of antifouling behaviours of modified PVDF membranes by TiO2sols with different nanoparticle size: Implications of casting solution stability. *J Memb Sci.* 525: 378-386. https://doi.org/10.1016/j.memsci.2016.12.021.

[32] F. N. A. M. Sabri, M. R. Zakaria, H. M. Akil. 2020. Dispersion and stability of multiwalled carbon nanotubes (MWCNTs) in different solvents. *AIP Conf Proc.* 2267. https://doi.org/10.1063/5.0024711.

[33] A. N. Omrani, E. Esmaeilzadeh, M. Jafari, A. Behzadmehr. 2019. Effects of multi walled carbon nanotubes shape and size on thermal conductivity and viscosity of nanofluids. *Diam Relat Mater*. 93: 96-104. https://doi.org/10.1016/j.diamond.2019.02.002.

[34] L. Boor, K. Victor, H. Raed, H. Nidal. 2013. A review on membrane fabrication: Structure, properties and performance relationship. *Desalination*. 326: 77-95.

[35] P. Sahu, S. Musharaf Ali, K. T. Shenoy, S. Mohan. 2019. Nanoscopic insights of saline

water in carbon nanotube appended filters using molecular dynamics simulations. *Physical Chemistry Chemical Physics.* 21: 8529-8542. https://doi.org/10.1039/c9cp00648f.

[36] M. Thomas, B. Corry. 2016. A computational assessment of the permeability and salt rejection of carbon nanotube membranes and their application to water desalination, Philosophical Transactions of the Royal Society A: Mathematical. *Physical and Engineering Sciences.* 374. https://doi.org/10.1098/rsta.2015.0020.

[37] K. Yang, L. J. Huang, Y. X. Wang, Y. C. Du, Z. J. Zhang, Y. Wang, M. J. Kipper, L. A. Belfiore, J. G. Tang. 2020. Graphene oxide nanofiltration membranes containing silver nanoparticles: Tuning separation efficiency via nanoparticle size. *Nanomaterials.* 10. https://doi.org/10.3390/nano10030454.

[38] L. Wu, X. Liu, G. Lv, R. Zhu, L. Tian, M. Liu, Y. Li, W. Rao, T. Liu, L. Liao. 2021. Study on the adsorption properties of methyl orange by natural one-dimensional nano-mineral materials with different structures. *Sci Rep.* 11. https://doi.org/10.1038/s41598-021-90235-1.

[39] M. Padaki, R. Surya Murali, M. S. Abdullah, N. Misdan, A. Moslehyani, M. A. Kassim, N. Hilal, A. F. Ismail. 2015. Membrane technology enhancement in oil-water separation. A review. *Desalination.* 357: 197-207. https://doi.org/10.1016/j.desal.2014.11.023.